Stem Cell Reports
Article

ISSCR

OPEN ACCESS

The Median Eminence, A New Oligodendrogenic Niche in the Adult Mouse Brain

Rina Zilkha-Falb,[1,2,*] Nathali Kaushansky,[1] and Avraham Ben-Nun[1,3]
[1]Department of Immunology, The Weizmann Institute of Science, Rehovot, Israel
[2]Present address: Neuroimmunology Laboratory, Multiple Sclerosis Center, Sheba Medical Center, Tel-Hashomer 5262100, Israel
[3]Dedicated in memory of Professor Avraham Ben-Nun, a great human being and a courageous scientist
*Correspondence: rina.falb@sheba.health.gov.il
https://doi.org/10.1016/j.stemcr.2020.04.005

SUMMARY

The subventricular zone (SVZ) of the lateral ventricles and the subgranular zone (SGZ) of the dentate gyrus in the hippocampus are known as neurogenic niches. We show that the median eminence (ME) of the hypothalamus comprises BrdU$^+$ newly proliferating cells co-expressing NG2 (oligodendrocyte progenitors) and RIP (pre-myelinating oligodendrocytes), suggesting their differentiation toward mature oligodendrocytes (OLs). ME cells can generate neurospheres (NS) *in vitro*, which differentiate mostly to OLs compared with SVZ-NS that typically generate neurons. Interestingly, this population of oligodendrocyte progenitors is increased in the ME from experimental autoimmune encephalomyelitis (EAE)-affected mice. Notably, the thrombospondin 1 (TSP1) expressed by astrocytes, acts as negative regulator of oligodendrogenesis *in vitro* and is downregulated in the ME of EAE mice. Importantly, transplanted ME-NS preferentially differentiate to MBP$^+$ OLs compared with SVZ-NS in *Shiverer* mice. Hence, discovering the ME as a new site for myelin-producing cells has a great importance for advising future therapy for demyelinating diseases and spinal cord injury.

INTRODUCTION

Adult neural stem cells (NSCs) are major candidates for regenerative therapies in demyelinating diseases. Myelin, provided by oligodendrocytes (OLs), is essential for the proper function of neurons in the central nervous system (CNS). Myelin loss occurs in many demyelinating diseases, such as multiple sclerosis (MS) and causes a variety of neurological disabilities in adults (Duncan and Radcliff, 2016; Lassmann, 2018). In demyelinating disease lesions OLs are lost and to promote functional recovery, lesions must be supplied with endogenous or transplanted myelinating cells (Blakemore et al., 2002; Chari and Blakemore, 2002; Jeffery et al., 1999). Oligodendrocyte progenitor cells (OPCs) marked by NG2, a chondroitin sulfate proteoglycan, and PDGFRα (platelet-derived growth factor receptor α) are recruited to demyelinated lesions (Chang et al., 2000; Redwine and Armstrong, 1998; Reynolds et al., 2001; Sim et al., 2002). Olig2, a basic-helix-loop-helix transcription factor, is strongly upregulated in OPCs under pathological conditions and demyelination in the adult CNS (Buffo et al., 2005; Fancy et al., 2004; Talbott et al., 2005).

NSCs have been found in two main neurogenic regions of the brain (Emsley et al., 2005); the subgranular zone (SGZ) of the dentate gyrus (DG) in the hippocampus (Altman and Das, 1965) and the subventricular zone (SVZ) of the lateral ventricles (LVs) (Gould, 2007; Lim and Alvarez-Buylla, 2016). Neurogenesis may also occur in other areas of the adult brain—albeit at lower levels (Seri et al., 2006; Taupin, 2006). Recently, a novel site of NSCs was reported in the circumventricular organs (CVO) (Bennett et al., 2009). To date, studies focused on neurogenic niches directed mainly to neurogenesis with less attention to characterizing oligodendrogenic niches.

Studies of oligodendrogenesis in white matter regions of adult rodent CNS, revealed spontaneous NG2 cell division and new OLs formation (Cerghet et al., 2006; Dimou et al., 2008; Horner et al., 2000; Komitova et al., 2009; Seri et al., 2006).

In contrast to multiple studies reporting spontaneous neurogenesis in various CNS disorders (Taupin, 2008) as well as in the murine model of MS, experimental autoimmune encephalomyelitis (EAE) (Aharoni et al., 2005), spontaneous oligodendrogenesis was barely reported (Nait-Oumesmar et al., 2008; Picard-Riera et al., 2002).

The generation of new OLs in the SVZ was investigated extensively (Brousse et al., 2015; Kazanis et al., 2017; Serwanski et al., 2018; Xing et al., 2014), however, their ability to participate in myelin repair has remained uncertain. Nevertheless, it is of great importance to characterize niches of OPCs for their regulation in pathological conditions or re-population *in vitro* for further therapy. In addition, a number of molecules/molecular pathways were reported to regulate neurogenesis; however, the mechanism that preferentially directs oligodendrogenesis versus neurogenesis and lineage commitment is not yet clear.

Here, we looked into brain sites in naive mice that are highly enriched with bromodeoxyuridine (BrdU)$^+$ newly proliferating cells. Of these, the median eminence (ME) was attractive for its exclusive oligodendrogenic fate. Identifying the ME as a site that preferentially hosts NG2 cells,

we studied *in vitro* the self-renewal potential of ME-NSCs and the preferential differentiation to OLs compared with SVZ-NSCs. Indeed, we characterized the oligodendrogenic fate of ME-resident BrdU$^+$ cells in naive and EAE mice. More practically, we studied their ability to differentiate toward mature MBP-producing OLs in *Shiverer* (*Shi*) mice, a model for demyelination. Comprehensively, we studied *in vitro* a potential role for thrombospondin 1 (TSP1) in regulating the oligodendrogenic versus neurogenic fate and compared the expression of TSP1 in SVZ and ME of naive with that of EAE mice.

We show that the ME of naive mice is enriched with BrdU$^+$ NG2$^+$ cells and that their number is increased in EAE mice. *In vitro*, ME-NSCs generate neurospheres (NSs) that mostly differentiate to OLs while SVZ-NSCs differentiate to neurons. In accordance, ME-NSCs preferentially differentiate to MBP$^+$ OLs after transplantation to the LV of *Shi* mice, compared with SVZ-NSCs that differentiate toward neurons. Our results show that TSP1 favors neuronal differentiation of ME-NSCs, while an antagonist of TSP1 (LSKL) preferentially directs toward OLs. Finally, analysis of TSP1 in EAE mice shows decreased expression in the ME (versus SVZ) compared with naive mice.

These findings suggest the ME as an exclusive oligodendrogenic niche, an endogenous pool of OPCs, to enhance generation of OPCs under pathological conditions. Indeed, this study suggests that TSP1 plays as negative regulator of oligodendrogenesis *in vitro*.

RESULTS

Characterization of OPCs in the ME of the Hypothalamus

Brains of 8-week-old naive mice were analyzed for regions enriched with newly generated NSCs. C57Bl/6J mice were injected daily with BrdU for 3 days and brains were scanned for BrdU-enriched regions (Figure 1A). Comparative analysis revealed that the cortex (Ctx) and the striatum contain a minor population of BrdU$^+$ cells compared with the CC, DG, and SVZ. Interestingly, another BrdU$^+$-enriched region was identified in the ME (Figure 1B). To characterize the identity of BrdU$^+$ cells in this region, brain sections of naive mice were stained for neuronal and oligodendrocyte progenitor markers. No staining was detected for the early neuronal progenitor marker (DCX) in the ME (Figure 1C), or for NeuN (not shown). Surprisingly, the ME contained a large number and high density of OPCs (NG2$^+$ BrdU$^+$) compared with the CC, DG, and SVZ (Figure 1D). The majority of these NG2$^+$ cells were also PDGFRa$^+$ (Figures 1E and S1). Quantitation of NG2$^+$ BrdU$^+$/mm^2 and their percentages indicated that the number and density of OPCs is markedly higher in the ME (608 ± 106 cells in ME compared with 400 ± 149 cells in DG, 290 ± 9.1 cells in SVZ and 73 ± 73 cells in CC; Figures 1F and 1G), suggesting that the ME of naive mice is rich with newly formed OPCs.

Cells Originated from the ME Generate NS and Differentiate to Neuronal/Oligo Progenitor Cells

ME cells were examined for self-renewal and assessed for their capability to generate NS compared with those from the SVZ (Figure 2A, schematic explanation). Interestingly, ME cells generated NS 3–4 weeks after plating, while SVZ-NS could be detected already 7 days after plating. Clearly, the ME-NS (Figure 2B), which contain many NG2$^+$ OPCs and few DCX$^+$ neuronal progenitors and GFAP$^+$ astrocytes, showed pronounced differentiation to oligodendrocyte lineage (Figure 2C) compared with SVZ-NS (Figures 2D and 2E). Quantitative analysis indicated that ME-NS express DCX 2 days after differentiation (4.2 ± 0.6% of DAPI$^+$ cells in ME-NS compared with 5.32 ± 1.1% in SVZ-NS), but that this neurogenic potential gradually decreases at days 4, 8, and 12 after differentiation and that markers of mature neurons (β-tubulin III and NF200) are poorly expressed as compared with SVZ-NS (Figure 2F). Analysis of cells that were differentiated to OPCs or mature OLs (Figure 2G) indicated that ME-NS preferentially differentiated to NG2$^+$ OPCs 2 days after differentiation (2.67 ± 0.65% compared with 1.58 ± 1.84% in SVZ-NS) and their number gradually increased at days 4, 8, and 12 after differentiation (6.8 ± 1.4%, 7.9 ± 0.7%, and 18.5 ± 6%, respectively) compared with differentiation from SVZ-NS (5.1 ± 2.8%, 4.82 ± 1.8%, and 8.64 ± 3.6%, respectively). Moreover, the number of MBP$^+$ mature OLs increased after 4, 8, and 12 days (13.4 ± 2.5%, 17.4 ± 4.2%, and 29.8 ± 3.4%, respectively) compared with differentiation from SVZ-NS (10.9 ± 0.85%, 16.1 ± 1.9%, and 15.2 ± 3.3%, respectively; Figure 2G). These results are confirmed by western blot (WB) of β-tubulin and MBP (Figure S2).

These results demonstrate the self-renewal capacity of ME cells and suggest that ME cells preferentially differentiate to OLs.

Increased Number of OPCs in the ME of EAE Mice

The self-renewal capacity of ME cells and their potential to generate OLs prompted us to study the effect of a pathological condition, such as EAE, on newly generated OLs in the ME. Immunostaining for BrdU$^+$ cells in the ME, CC, and DG clearly showed that EAE induced cell proliferation in these regions and especially in the ME compared with these regions from naive mice, and that a fraction of these BrdU$^+$ cells was also NG2$^+$ (Figure 3A, left panel), which was increased in EAE mice as compared with naive mice. In contrast, there was no evidence of DCX$^+$ cells in

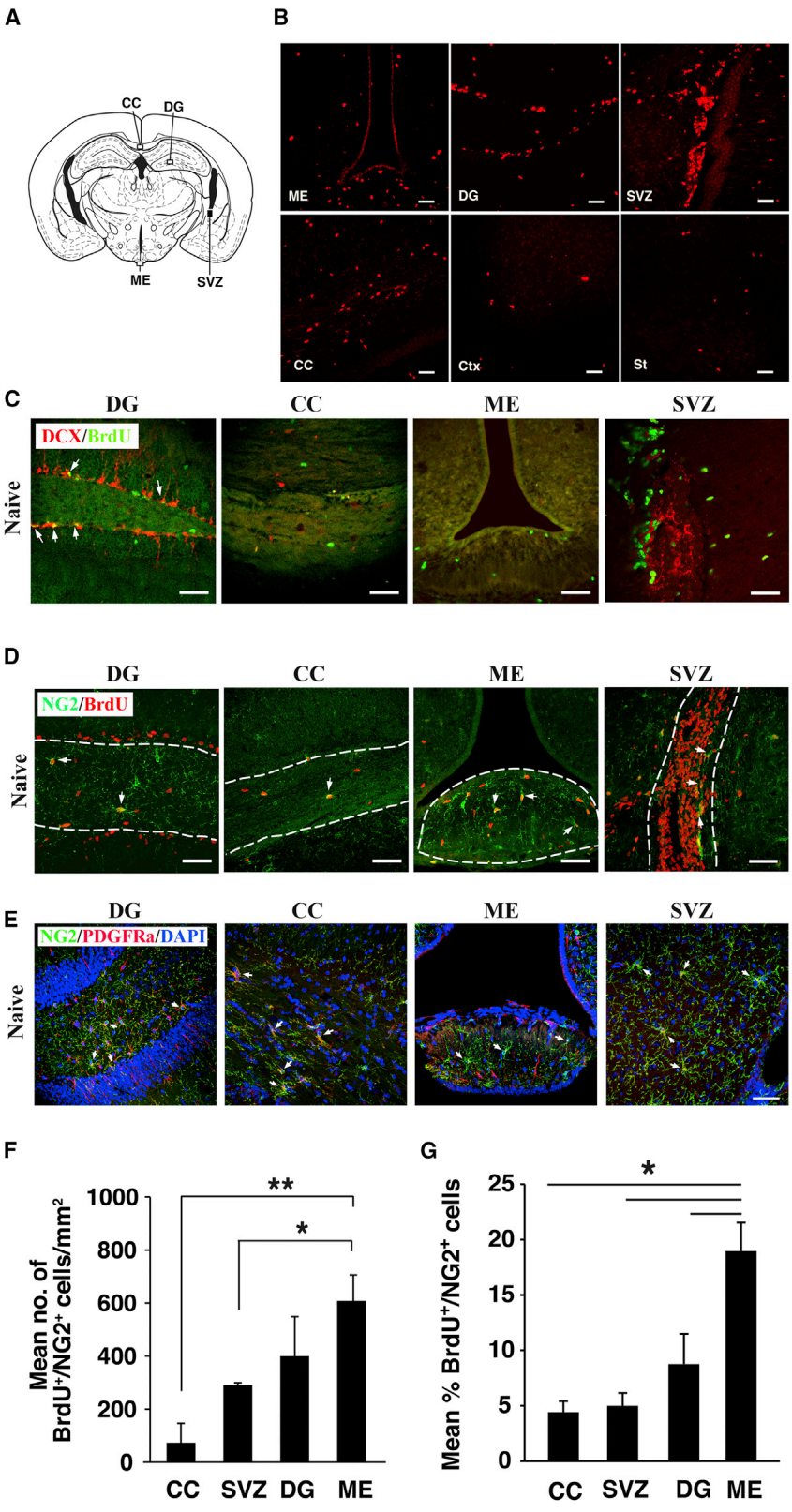

Figure 1. OPCs in the ME of Naive Mice

(A) Scheme shows regions analyzed for $BrdU^+$ cells.

(B) BrdU staining in the ME DG, SVZ, CC, Ctx, and St.

(C) Absence of neuronal progenitors (DCX) in the ME and CC compared with DG. Arrows indicate DCX^+ $BrdU^+$ cells.

(D) Images show OPCs (NG2) in the DG, CC, SVZ, and ME boxed in (A). Arrows indicate $NG2^+$ $BrdU^+$ cells.

(E) Images show $NG2^+$ $PDGFRa^+$ OPCs.

(F and G) Quantitative analysis of $NG2^+$ $BrdU^+$ cells in the DG, CC, SVZ, and ME as (F) mean number of $NG2^+$ $BrdU^+$ cells/mm^2. *p = 0.013, **p = 0.00079, and (G) as their mean percentage of $BrdU^+$. *p = 0.0007 (n = 4 for each group).

Scale bar, 50 μm.

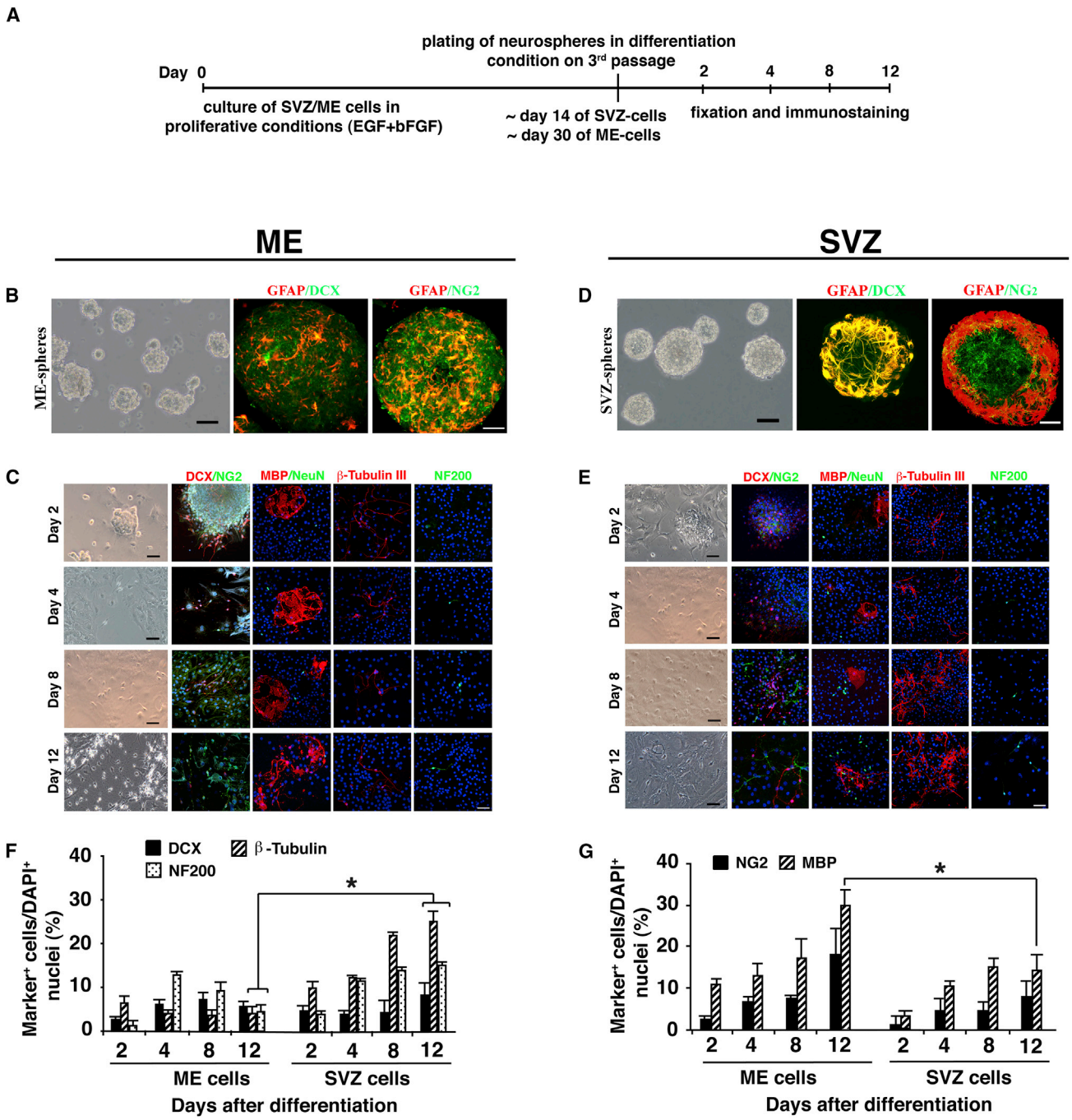

Figure 2. ME Cells Generate NS and Differentiate *In Vitro* to Neuro/Oligo Progenitors

(A) Explanation of NS culture and fixation schedule.

(B and D) Generation of NS from (B) isolated ME compared with (D) SVZ cells. Expended ME-NS express markers of neuronal (DCX), oligodendrocyte progenitors (NG2), and astrocytes (GFAP). Shown are bright field images of NS and immunostaining for neural markers.

(C and E) Temporal analysis of neural markers expressed by ME-NS (C) upon differentiation compared with (E) SVZ-NS and their quantitative analysis of (F) neuronal and (G) oligodendrocyte markers (G).

Scale bar, 50 μm.

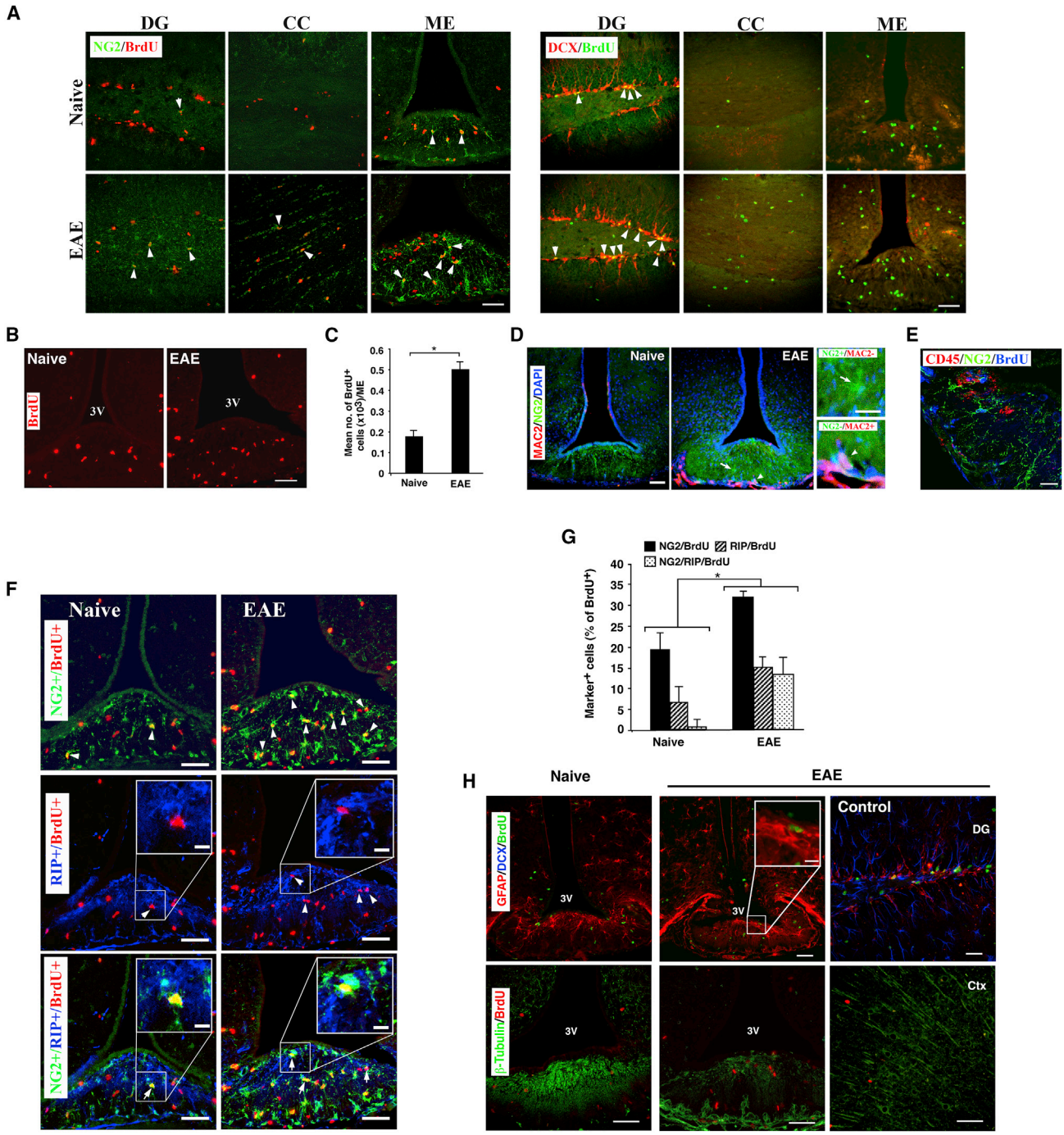

Figure 3. Increased Number of OPCs in the ME of EAE Mice

(A) Images show NG2/BrdU and DCX/BrdU staining in the DG, CC, and ME.

(B) Enhanced BrdU staining of ME in EAE mice compared with naive mice. Arrows indicate double-positive cells.

(C) Increased $BrdU^+$ cells in EAE mice compared with naive mice (n = 5 per group).

(D) Macrophages ($MAC2^+$) are not localized where OPCs are scored.

(E) $NG2^+$ cells are distinctive from $CD45^+$ cells.

(F and G) (F) Images of $BrdU^+$ $NG2^+$, $BrdU^+$ RIP^+ (arrowheads), and $BrdU^+$ $NG2^+$ RIP^+ cells (arrows) in the ME of EAE mice and (G) their quantitative analysis (n = 4 per group).

(H) Immunostaining for DCX or β-tubulin with BrdU in the ME.

Scale bar, 50 μm. (C) *p < 0.01, (G) *p = 0.02.

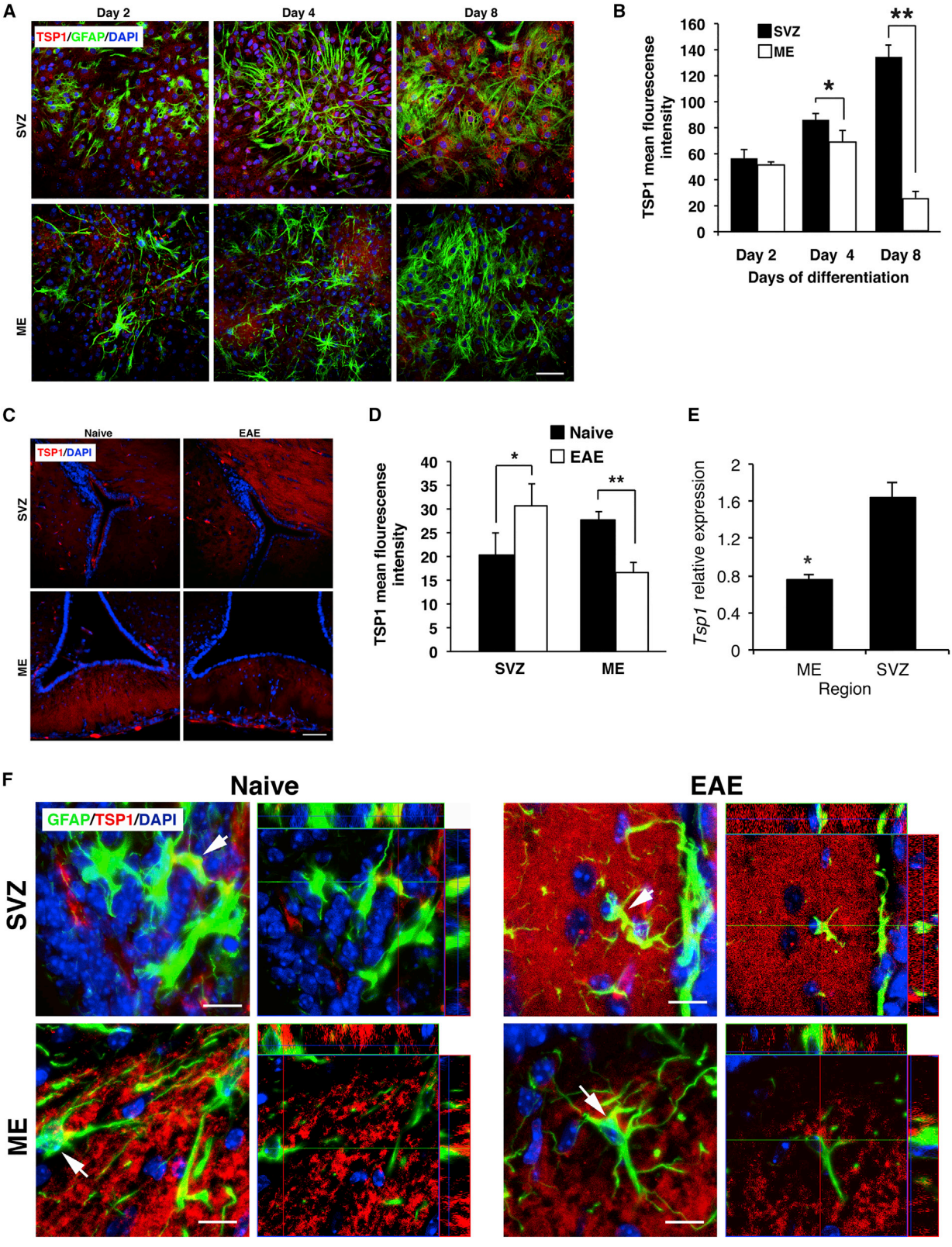

(legend on next page)

the ME and CC compared with DG, although there was an increased number of $BrdU^+$ cells (Figure 3A, right panel). Higher-magnification images of $BrdU^+$ cells in the ME clearly showed that, under EAE, an increased cell proliferation was detected compared with the same region in naive mice (Figure 3B). The mean number of $BrdU^+$ cells per ME was increased (by 2.7-fold; $p < 0.01$) in EAE mice compared with naive mice (Figure 3C). Staining for macrophages and OPCs (Figure 3D) excluded the possibility that these parenchymal resident $BrdU^+$ cells were immune cells that penetrated the CNS as the $MAC2^+$ cells resided at the edge of ME tissue but not in the parenchyma where the $BrdU^+$ cells were detected (Figure 3D). Moreover, the immune cell marker, CD45 staining, excluded the possibility that the $NG2^+$ $BrdU^+$ cells were infiltrating immune cells (Figure 3E). To characterize these newly generated cells, adjacent sections were immunostained for markers of OLs. Comparison of sections from EAE mice to sections of naive mice showed that $BrdU^+$ cells expressed NG2 (Figure 3F, upper panel) or RIP of pre-myelinating OLs (Figure 3F, middle panel) and that their number was increased in EAE mice, while a comparable intensity of MBP immunoreactivity in the ME of naive and EAE mice was observed (Figure S4A).

Moreover, numerous $BrdU^+$ cells expressed both NG2 and RIP in sections from EAE mice compared with those from naive mice (Figure 3F, lower panel). The percentage of $NG2^+$ $BrdU^+$ and RIP^+ $BrdU^+$ cells increased in the ME of EAE mice by 13% and 8.4%, respectively. Moreover, a marked increase in the percentage of $NG2^+$ RIP^+ $BrdU^+$ in EAE mice could be observed (Figure 3F). Of note, ME sections from EAE or naive mice showed neither $BrdU^+$ co-expressing β-tubulin III nor DCX compared with such positive staining in the Ctx (Figure 3H). A small number of $GFAP^+$ $BrdU^+$ cells could be detected in the ME of EAE mice (Figure 3H). Notably, such oligodendrogenesis can be observed in the ventro-medial region (VMH) and the arcuate nucleus (Arc) of the hypothalamus, but to a lesser extent, and obviously the number of $NG2^+$ $BrdU^+$ cells is significantly higher in the ME of naive and EAE mice compared with the Arc and VMH (Figure S3).

These results suggest that EAE extensively promotes oligodendrogenesis in the ME.

Expression of TSP1 by NSCs *In Vitro* and Spatial Analysis of TSP1

TSP1 was implicated in the direction of SVZ-NSCs toward neuronal differentiation (Lu and Kipnis, 2010), raising the possibility that TSP1 may act as negative regulator of oligodendrogenesis in ME. Hence, we compared the expression of TSP1 by SVZ-NSCs with that of ME-NSCs. Expression of TSP1 could not be detected in NS of ME or SVZ (data not shown). However, as shown in representative images (Figure 4A) and by quantitative analysis (Figure 4B), its expression in the ME was upregulated 2 and 4 days after differentiation and then significantly declined after 8 days. In contrast, expression of TSP1 in SVZ-NSCs was only slightly increased at days 2 and 4 after differentiation but increased after 8 days. In brain sections, TSP1 expression was decreased in ME of EAE mice compared with naive mice. However, TSP1 level in the SVZ was increased (Figure 4C), and the mean fluorescent intensity (MFI) confirmed these differences in TSP1 expression (Figure 4D). The MFI showed 1.5-fold increase in the SVZ of EAE mice compared with naive mice ($p = 0.003$), while there was 1.8-fold decrease in the ME of EAE mice compared with naive mice ($p < 0.001$; Figure 4D). *Tsp1* relative expression in EAE mice was decreased by 2-fold in ME ($p = 0.04$; Figure 4E) compared with naive mice. Moreover, $GFAP^+$ immunostaining indicated decreased TSP1 expression (control staining; Figure S4B) by astrocytes in ME of EAE mice compared with naive mice and increase in the LV of EAE mice (Figures 4F and S4C, low power images).

Effect of TSP1 on Differentiation of NSCs from SVZ versus ME and Expression of TSP1 by NSCs

The increased number of OPCs in the ME of EAE mice and the decreased TSP1 expression hints on the role of TSP1 as negative regulator of oligodendrogenesis. To study this possibility, SVZ- or ME-NSCs were differentiated for 8 days in the absence or presence of TSP1 or bovine serum albumin (BSA) as a control (both at 2 μg/mL) and cultures were stained against NG2 and DCX (Figure 5A, schematic explanation). Incubation with TSP1 resulted in significantly reduced number of $NG2^+$ OPCs differentiated from both SVZ- and ME-NSCs, especially in ME-NSCs compared with BSA or vehicle control (Figure 5B). Inversely, addition of TSP1 increased the number of neuronal progenitors in

Figure 4. Expression of TSP1 by ME- and SVZ-NSCs

(A and B) (A) Immunostaining for GFAP and TSP1 after the indicated time points of differentiation and (B) quantitative analysis of TSP1 fluorescence intensity ($n = 6$).

(C) Images of immunostaining for TSP1 in SVZ and ME.

(D) Quantitative analysis of TSP1 fluorescence intensity in SVZ and ME ($n = 4$ per group). *$p = 0.003$, **$p = p < 0.001$.

(E) *Tsp1* relative expression in the ME and SVZ. *$p = 0.036$.

(F) Orthogonal views of GFAP and TSP1 in ME and SVZ in naive mice compared with EAE mice. Low-power images of TSP1 are shown in Figure S4C. Scale bar, 50 μm.

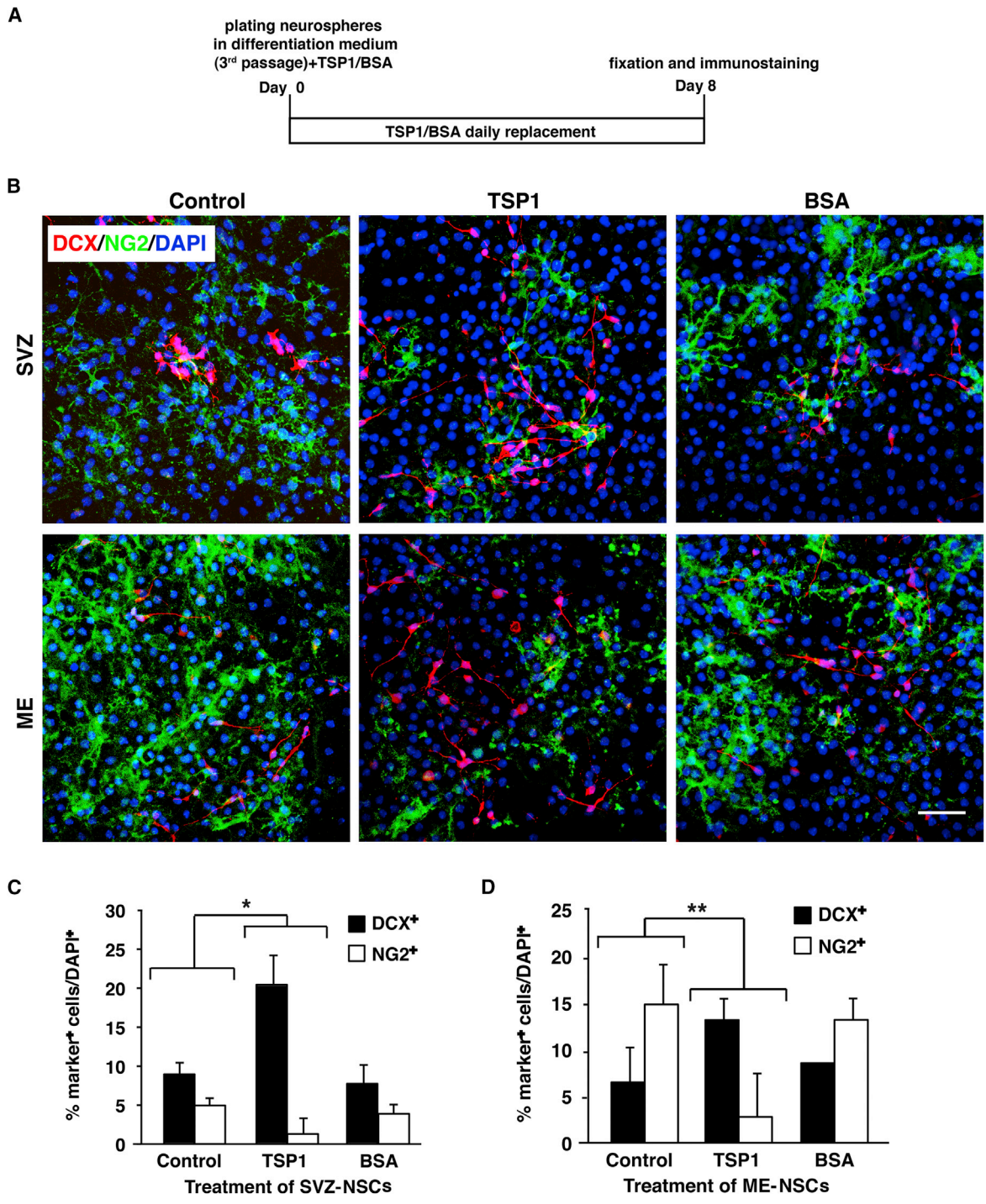

Figure 5. Effect of TSP1 on Differentiation of ME-NSCs Compared with SVZ-NSCs

(A) Explanation of NS culture, differentiation in presence of TSP1, and fixation schedule.

(B) Staining for DCX and NG2 in ME- and SVZ-NSCs cultures treated with TSP1 or BSA. NSCs cultured in differentiation medium served as control. Shown are representative images out of three repeats.

(C and D) Quantitative analysis of (C) SVZ-NSC and (D) ME-NSC differentiation to DCX^+ cells and $NG2^+$ cells in the presence of TSP1 (mean ± SD). Scale bar, 50 μm. *$p \leq 0.004$, **$p \leq 0.005$.

ME-NSCs and dramatically in SVZ-NSCs. Quantitative analysis showed that incubation with TSP1 increased the number of DCX$^+$ neuronal progenitors differentiated from SVZ-NSCs by 12% and decreased NG2$^+$ OPCs by almost 4% (Figure 5C).

A similar effect could be detected in differentiation of ME-NSCs, where TSP1 increased the number of neuronal progenitors by 8.2% and dramatically decreased the number of OPCs (by ~13%) relative to control cultures (Figure 5D). A WB for the neuronal β-tubulin and oligodendroglial GST-pI confirmed these results (Figure S5).

TSP1 Antagonist Shifts NSC Differentiation toward OPCs

To further confirm a role for TSP1 as a negative regulator of oligodendrogenesis *in vitro*, we studied the differentiation of ME-NSCs compared with SVZ-NSCs in the presence of TSP1 antagonist LSKL, a 4-amino acid peptide that specifically blocks the binding of TSP1 and the large latent transforming growth factor β (TGF-β) complex (Lanz et al., 2010). ME- or SVZ-NSCs were differentiated in the presence of LSKL or its control-scrambled peptide SLLK (50 μg/mL) and labeled for NG2 and DCX (Figure 6A, schematic explanation). Incubation with TSP1 antagonist increased the number of OPCs differentiated from both SVZ- and ME-NS, especially in SVZ-NSCs. Inversely, the TSP1 antagonist reduced the number of neuronal progenitors in ME- and SVZ-NSCs (Figure 6B). Quantitative analysis showed that incubation with the TSP1 antagonist significantly increased the number of NG2$^+$ OPCs differentiated from SVZ-NSCs by 7%, and decreased the number of DCX$^+$ neuronal progenitors by almost 4% (Figure 6C). Similarly, the TSP1 antagonist increased the number of NG2$^+$ OPCs differentiated from ME-NSCs by almost 3%, and decreased the number of DCX$^+$ neuronal progenitors by 2.4%, compared with control cultures (Figure 6D). A WB for the neuronal β-tubulin and oligodendroglial GST-pI confirmed these results (Figure S6). Altogether, these results further suggest that TSP1 negatively regulates oligodendrogenesis *in vitro*.

ME-Originated Cells Preferentially Generate MBP$^+$ OLs in the CNS of *Shi* Mice

The *in vitro* results show that ME-NS can differentiate to mature MBP$^+$ OLs (Figure 2), express chemokine receptor for migration, and provide neurotrophic support (Figures S7A and S7B). To unambiguously determine whether grafted ME-NSCs become fully mature myelinating OLs, ME-NSCs derived from GFP mice were grafted into the LV of *Shi* mice lacking MBP (Warrington et al., 1993). Hence, MBP labeling in their brain can only come from grafted cells.

Two-week-old *Shi* mice were transplanted with either ME- or SVZ-NS (n = 4 per group). At 3 weeks post-grafting, GFP$^+$ cells derived from ME-NS had migrated and were found mainly in the CC and rarely in LV, while GFP$^+$ cells derived from SVZ-NS were detected mainly in the LV and in the parenchyma in the vicinity of the LV (Figure 7A). These results confirm the ability of adult SVZ- and ME-NS to survive in the LV and CC of *Shi* mice, respectively, after migration and differentiation. Higher-magnification images showed GFP$^+$ cells derived from ME-NS in the CC that co-express MBP. Such GFP$^+$ MBP$^+$ cells could be observed also in the parenchyma at the vicinity of LV but to a lower extent. The pattern of MBP labeling indicated that grafted cells had formed myelin patches throughout the CC (Figures 7B, upper set of panels and S7C) with process-bearing ramified GFP$^+$ cells that co-express MBP (Figure 7B, inset in upper right set of panels). As shown in Figure 7B (middle set), only a small number of GFP$^+$ cells derived from ME-NS also expressed DCX in the CC. In addition, although these GFP$^+$ cells were detected at the vicinity of LV, none co-expressed DCX. Analysis the fate of SVZ-NS showed that only few GFP$^+$ cells derived from SVZ-NS co-expressed MBP in the CC (Figure 7C, upper left set of panels), a typical niche of OLs, while no MBP$^+$ GFP$^+$ cells could be detected in the LV (Figure 7C, lower left set of panels). However, while only few GFP$^+$ cells derived from SVZ-NS co-expressed the neuronal marker DCX in CC (Figure 7C lower right set of panels), the frequency of such cells was higher in the parenchyma near the LV with a morphology reminiscent of neurons (Figure 7C, inset in upper right set of panels).

Quantification 3 weeks after transplantation showed that 32.9 ± 8.8% of GFP$^+$ cells derived from ME-NS co-expressed MBP. Most of them were detected in the myelinogenic area, such as the CC, while only 0.8% co-expressed the neuronal marker DCX and were detected near the LV (Figure 7D). Inversely, only 3.1 ± 6% of GFP$^+$ cells derived from SVZ-NS co-expressed MBP$^+$, while 29 ± 9% of these cells co-expressed DCX and were mostly detected in the vicinity of the LV (Figure 7D). These results suggest that ME-NS preferentially generate OLs in adult subcortical white matter after a heterotopic graft compared with SVZ-NS and that oligodendrogenic or neurogenic fate chosen by NS depended not only on the environment cues encountered in the host regions but also on intrinsic features of the cells origin.

DISCUSSION

Here, we show that the ME of naive mice is enriched with BrdU$^+$ cells identified as NG2$^+$ cells and that the number of these BrdU$^+$ NG2$^+$ cells is increased in the ME of EAE mice. Interestingly, these cells can generate NS *in vitro*. In line with the *in situ* observation, ME-NSCs mostly differentiate to OLs upon *in vitro* differentiation. In accordance,

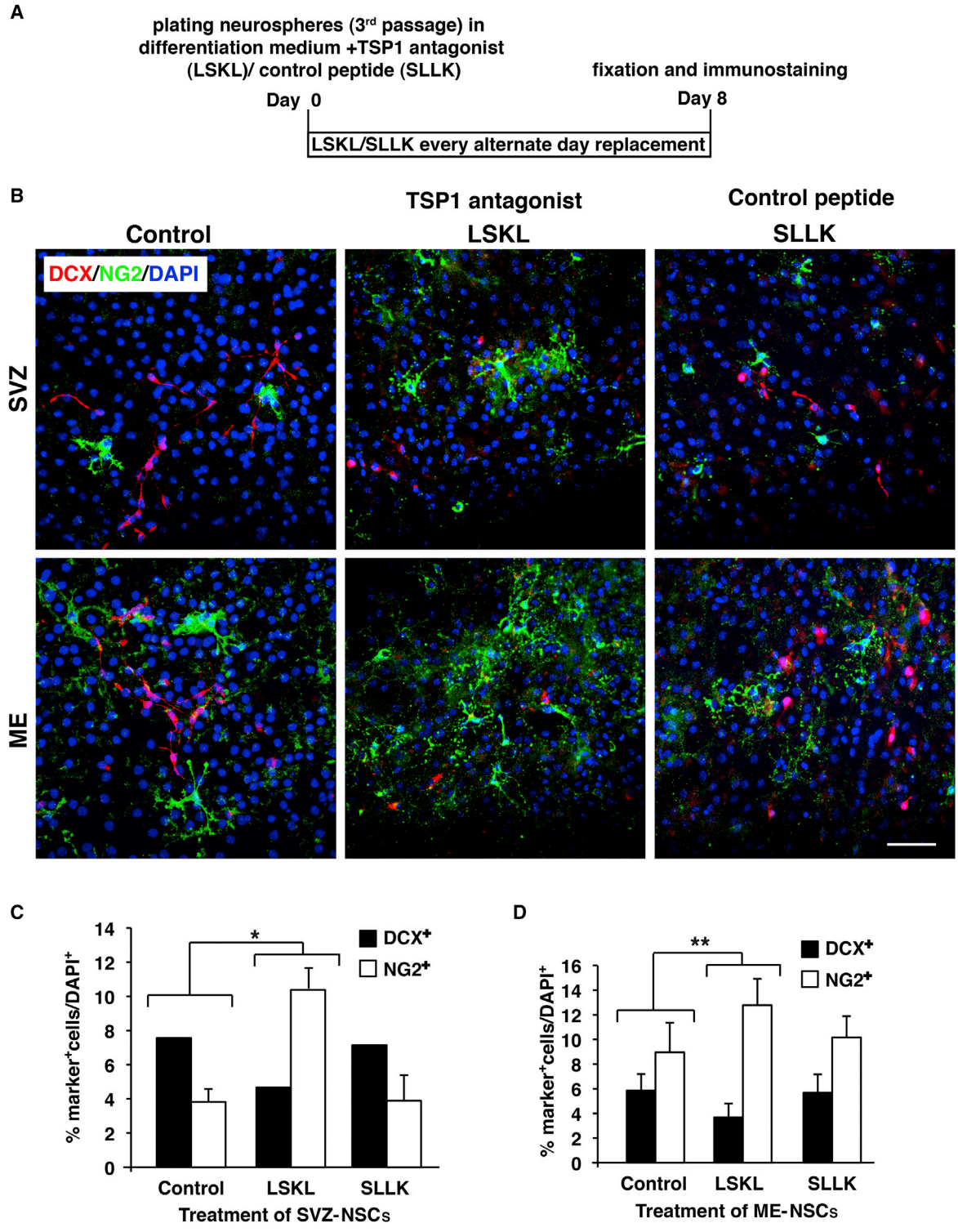

Figure 6. Effect of TSP1 Antagonist on Differentiation of ME-NSCs Compared with SVZ-NSCs

(A) Explanation of NS culture, differentiation in the presence of TSP1 antagonist or control peptide and fixation schedule.

(B) Staining for DCX and NG2 in ME- and SVZ-NSCs cultures treated with TSP1 antagonist (LSKL) or control peptide (SLLK) (50 μg/mL).

(C and D) Quantitative analysis of (C) SVZ-NSCs and (D) ME-NSCs differentiation to DCX^+ and $NG2^+$ cells in the presence of TSP1 antagonist (mean ± SD). Scale bar, 50 μm. *$p \leq 0.004$, **$p \leq 0.015$.

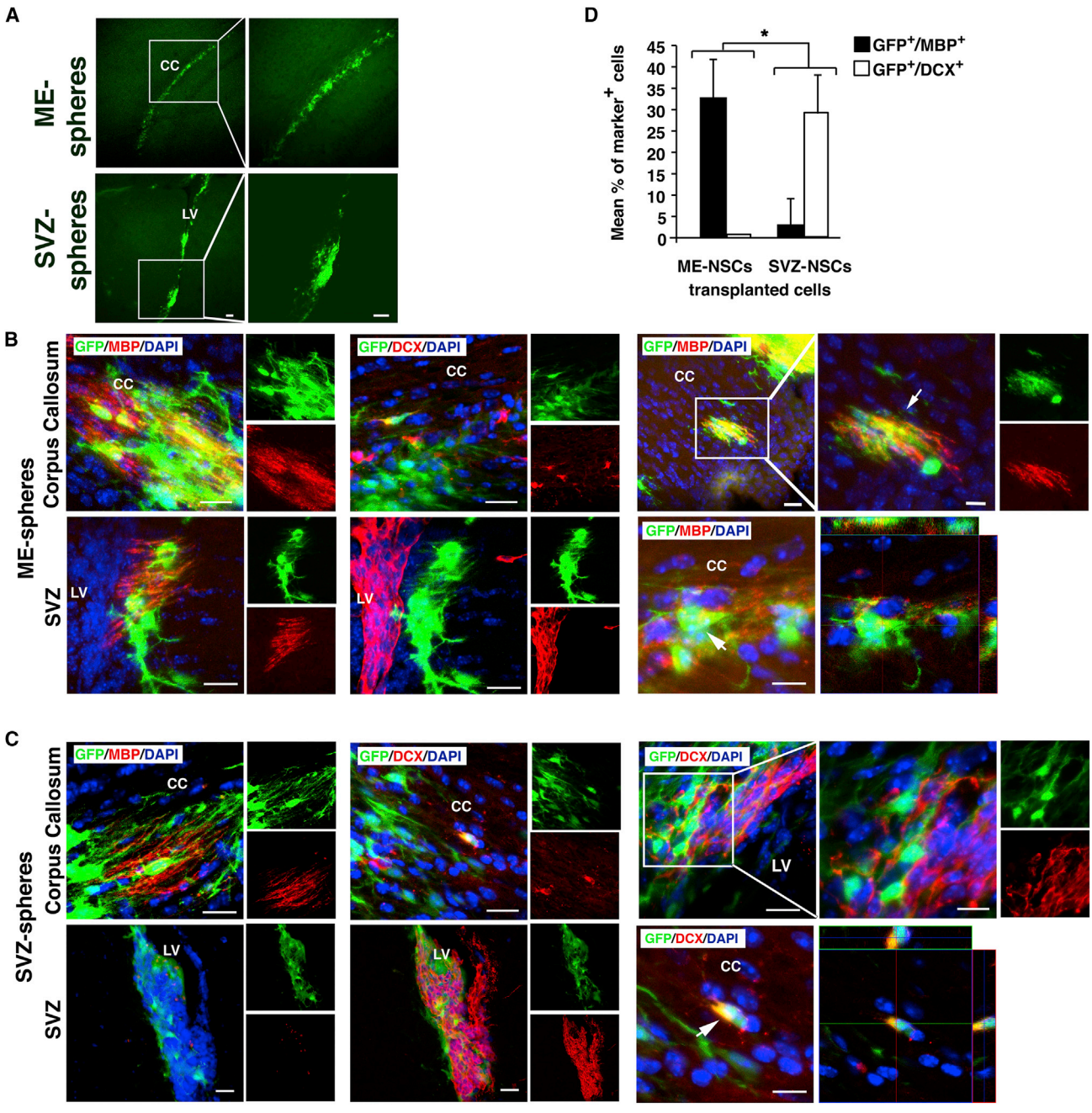

Figure 7. ME-Derived OLs Express MBP in *Shi* Mice

Coronal brain sections processed 3 weeks after injection of GFP-labeled NS into the LV.

(A) Images show GFP^+ ME-NS (upper panel) or GFP^+ SVZ-NS.

(B) Images show transplanted GFP^+ ME-NSCs in the ME (upper panel) and SVZ (lower panel) expressing MBP (left column) or DCX (middle column). Upper images in the right column show higher magnification of GFP^+ MBP^+ in the CC. Scale bars, 20 μm and 10 μm (inset). The lower image is an orthogonal view showing localization of MBP with GFP^+ ME-NSCs. Scale bar, 10 μm.

(C) Images show GFP^+ SVZ-NSCs in the CC (upper panel) and adjacent LV (lower panel). Shown are immunostaining for MBP (left column) and DCX (middle column). Upper images in the right column show higher magnification of GFP^+ DCX^+ in the SVZ. Scale bars, 20 μm and 10 μm (inset). The lower image is orthogonal view showing localization of DCX with GFP^+ SVZ-NSCs. Scale bar, 10 μm.

(D) Quantitative analysis of GFP^+ cells co-express MBP or DCX in *Shi* mice transplanted with ME-NSCs compared with SVZ-NSCs (n = 5 per group). Scale bars, 50 μm (A–C). *$p < 0.001$.

these ME-NSCs preferentially differentiate to MBP$^+$-producing OLs after transplantation to the LV of *Shi* mice. Mechanistically, our results show that TSP1 favors neuronal differentiation of ME-NSCs, while the TSP1 antagonist preferentially directs differentiation to OLs. Finally, analysis of TSP1 expression in EAE mice shows decreased expression in the ME (versus SVZ) compared with naive mice, which is in accordance with the effect of TSP1 *in vitro*.

These findings suggest that the ME is an exclusive oligodendrogenic niche that can serve as an endogenous pool of OPCs, and as a target to enhance the generation of OPCs under pathological conditions. Indeed, this study suggests that TSP1 plays a negative regulator of oligodendrogenesis *in vitro*.

Our study shows that the ME, considered as a CVO (Ganong, 2000), is enriched with BrdU$^+$ cells both in naive and to a greater extent in EAE mice, can generate NS and differentiate to neurons and OLs, as described previously (Bennett et al., 2009; Lin and Iacovitti, 2015; Robins et al., 2013a, 2013b). Interestingly, ME-NSCs preferentially differentiate to OLs, corroborated by the *in vivo* results showing that BrdU$^+$ cells in the ME are NG2$^+$, while no immunoreactivity for neuronal marker with BrdU$^+$ can be detected. BrdU$^+$ NG2$^+$ cells in the ME may represent a pool of latent progenitors, which are relatively quiescent in the brain of naive mice, yet possess the potential to proliferate and differentiate under specific circumstances. In this regard, like other CVOs, with their abundance of fenestrated capillaries and their proximity to ventricles, the ME may be ideally positioned to response to pathological conditions such as inflammation, stroke (Lin and Iacovitti, 2015), traumatic brain injury (Falnikar et al., 2018), or physiological cues, suggesting that signaling factors present in blood may be relevant to stimulating the ME niche to generate OPCs. In support of this notion, Kokoeva et al. (2005) showed that ciliary neurotrophic factor robustly induces cell proliferation in the hypothalamus.

An interesting issue is the physiological significance of the increased OPCs in the ME, which was mainly studied with respect to energy balance, weight loss, and nutritional signaling (Djogo et al., 2016; Kohnke et al., 2019), but not with demyelinating conditions.

In the pathological context, our findings of increased number of OPCs in the ME of EAE mice, and particularly their differentiation to pre-myelinating OLs and MBP$^+$ cells, suggest these OPCs as a backup pool to replace mature OLs that turnover with time, for OLs that support sensory neurons and essential for balance of body energy and metabolism rather than represent a transient population with myelin-unrelated roles.

Hence, our study suggesting the role of these OPCs during myelin repair further shed light on the pathological context of OPCs pool in the ME.

As a CVO, the ME is exposed to many factors that may maintain stem cells under normal physiological conditions and, like known neurogenic SVZ and SGZ regions, the ME microenvironment may possess factors critical for maintaining progenitors and regulating differentiation (Falnikar et al., 2018). Similarly, numerous studies show that dehydration stress (Virard et al., 2008) or demyelination (Picard-Riera et al., 2002) promote proliferation of OPCs. In line with our findings, recent studies demonstrated enhanced proliferation in the ME in a stroke model, however, and interestingly the proportion of differentiating neurons was significantly increased after focal ischemic stroke (MCAO) compared with OLs and astrocytes, representing a shift toward neurogenesis in the injured brain (Falnikar et al., 2018; Lin and Iacovitti, 2015). This raises the possibility of niche plasticity and differentiation on demand upon injury. Intriguingly, we could not detect neuronal progenitors in the ME as shown previously (Lin and Iacovitti, 2015; Robins et al., 2013a, 2013b). These differences could be attributed to methodological disparities between studies.

Our data suggest that the ME predominantly give rise to OPCs and OLs in healthy brain, which is enhanced in demyelinating condition. Such remyelination capacity of SVZ-NSCs was demonstrated in an EAE model (Pluchino et al., 2003) and of OPCs from human fetal forebrain transplanted in *Shi* mice (Windrem et al., 2004).

Although we did not track the origin of OPCs lining the ME, recent findings evidently suggest that stem cells in this region do not migrate there from other areas of high stem cell proliferation (i.e., SVZ) and instead the third and fourth ventricles are likely novel niches for stem cell production (Lin and Iacovitti, 2015).

Beside the SVZ and SGZ, neurogenesis may occur in other areas of the adult brain; CA1 (Rietze et al., 2000), neocortex (Gould et al., 1999, 2001), striatum (Bedard et al., 2002), amygdala (Bernier et al., 2002), substantia nigra (Zhao et al., 2003), third ventricle (Xu et al., 2005), subcortical white matter (Luzzati et al., 2006), caudate nucleus (Takemura, 2005), and leptomeninges (Bifari et al., 2009). However, regions of oligodendrogenesis except for Ctx were purely characterized (Naruse et al., 2017; Winkler et al., 2018). Virard et al. (2008) showed that the adult neurohypophysis contains glial progenitors capable of differentiating into OLs but the structure does not harbor NSCs. Picard-Riera et al. (2002) showed that EAE associated with demyelination enhances proliferation in SVZ and promotes mobilization of SVZ cells to demyelinated white matter structures, generating neurons and OLs. Seri et al. (2006) reported that cells isolated from the SCZ and cultured as NS behave as NSCs *in vitro* and migrate into the CC to become OLs *in vivo*.

These studies support our data showing the oligodendrogenic fate of newly generated cells in the ME of naive mice.

Moreover, this oligodendrogenesis is enhanced in EAE mice. Our finding that these newly generated cells in the ME can be detected in naive mice (also shown by Robins et al., 2013b) and express the RIP marker of pre-myelinating OLs suggests that these cells do not migrate from other neurogenic regions but represent ME-resident cells with proliferation capacity. It is intriguing if the ME is exclusively oligodendrogenic as shown here, although a low percentage of neuronal progenitors differentiated from ME-NS could be detected *in vitro*, which may result from the lack of the *in vivo* environmental cues characterizing the ME. In accordance with this notion, Komitova et al. (2009) shows that fewer than 1% of proliferating cells in the SVZ are NG2 cells which are more abundant in the nonneurogenic parenchyma, suggesting that $NG2^+$ OPCs are distinct from cellular constituents of the SVZ known as type A, B, or C cells (Alvarez-Buylla et al., 2002) and that the SVZ is mostly neuronogenic. Consistently, our study strongly suggests that the ME is an oligodendrogenic rather than an neuronogenic niche, corroborated by the absence of $BrdU^+$ cells co-expressing markers of neuronal progenitors in the ME.

As with neurogenesis (Lin and Iacovitti, 2015), the production of OLs is restricted (Moyse et al., 2008), demonstrated to arise from the tissue microenvironment, which led to the emerging concept of an "oligodendrogenic niche." However, the possibility that neuro/oligodendrogenesis is directed by combination of both extrinsic and intrinsic factors should be considered as well. The adult neural parenchyma contains a widely distributed potential for oligodendrogenesis that is not expressed in standard conditions, but which may be recruited for brain repair (Buffo, 2007). It could be speculated that niche-dependent differences are mediated by adaptations of OPCs to their environment by reacting to local signaling (van Tilborg et al., 2018).

Astrocytes induce formation of excitatory synapses by secreting TSP1/2 (Christopherson et al., 2005). Our results showing that SVZ-residing astrocytes of EAE mice express high level of TSP1 are consistent with the evidence that reactive astrocytes showing increased expression of TSP1, suggesting that these astrocytes are likely A2 type.

TSP1 was proposed to play a role in neuronal differentiation but inhibit differentiation of SVZ-NS toward OLs (Lu and Kipnis, 2010). Consistently, our *in vitro* and *in vivo* data suggest that astrocytic TSP1 plays a negative regulator of the oligodendrogenic fate of ME-NSCs both as an intrinsic and an extrinsic factor. Notably, TSP1 staining in the brain appears widely and diffusely, suggesting that there might be another source than just the astrocytes, likely neurons (Tyzack et al., 2014) and activated microglia (Rivera et al., 2017), which are highly abundant under neuroinflammation. In this study, LSKL, which blocks the binding of TSP1 and the large latent TGF-β complex, antagonized the effect of TSP1, suggesting that the effect of TSP1 is mediated by TGF-β. This notion is further sustained by the decreased expression of TSP1 in the ME of EAE mice associated with increased number of OPCs.

While the SVZ-NSCs mostly generate neuronal lineage and only a few OLs with some lineage plasticity in pathological conditions (Armada-Moreira et al., 2015), our study demonstrates the oligodendrogenic potential of the ME both *in vitro* and *in vivo* and the role of TSP1 as a negative regulator of oligodendrogenesis *in vitro*. Our findings suggest the ME niche as a pool of "backup" OPCs that can differentiate in the case of injury to surrounding OLs and as a target for enhancement of oligodendrogenesis while devising therapies for demyelination diseases.

EXPERIMENTAL PROCEDURES

Animals

C57Bl/6J and SJL/J mice were purchased from Jackson Laboratory (Bar Harbor, ME, USA) or obtained from the Weizmann Institute colony. (C57Bl/6J x SLJ/J)F1 mice were bred at the Weizmann Institute Animal Facility. *Shi* mice were purchased from Jackson Laboratory. All animals were handled according to the regulations formulated by the Institutional Animal Care and Use committee of the Weizmann Institute (permit no. 02820711-3) and were performed in compliance with its relevant guidelines and regulations.

Reagents and Antibodies

The mouse PLP139-151 peptide was synthesized in the laboratory of Prof. M. Fridkin (Department of Organic Chemistry, The Weizmann Institute of Science), using the Fmoc technique with an automated peptide synthesizer (AMS422; Abimed, Langenfeld, Germany). For list of antibodies see Table S1.

Active Induction of EAE

$(C57Bl/6J \times SJL/J)F_1$ mice (6- to 8-week-old female) were immunized, observed, and scored as described previously (Zilkha-Falb et al., 2016).

Administration of BrdU and Tissue Processing

When reached a maximal clinical score (3) usually at day 20 post-immunization, mice were injected i.p. with BrdU (Sigma-Aldrich; 50 mg kg^{-1} body weight) daily for 3 days and then were sacrificed. Animals were deeply anesthetized with a xylazine/ketamine mixture and perfused intracardially with cold 4% paraformaldehyde (PFA). Brains were postfixed in 2% PFA and cryoprotected in a 15% sucrose solution. Free-floating sections (30 μm thick) were cut coronally with a sliding microtome (Leica SM, 2000r; Leica, Nussloch, Germany).

NSCs Culture from SVZ and ME

NSCs were generated from the SVZ of the LV or the ME of the hypothalamus from brains of C57Bl/6J mice (6–8 weeks old) as described (Zilkha-Falb et al., 2016). For fate tracking, ME- and SVZ-NSCs were generated from GFP mice (kindly provided by the

lab of Michal Schwartz, Department of Neurobiology, The Weizmann Institute of Science). NS were differentiated by plating on poly-D-lysine (PDL) (Sigma-Aldrich, Rehovot, Israel), in growth factor-free NS medium containing 3% serum (differentiation medium). For immunocytochemistry, cells were plated on PDL-coated coverslips. To study the effect of TSP1, NS were differentiated in the presence of 2 μg/mL TSP1 (kindly provided by the lab of Prof. Jonathan Kipnis, University of Virginia, Charlottesville, VA, USA) or BSA, and replaced everyday with fresh TSP1 and BSA for 8 days. To study the effect of TSP1 antagonist LSKL and its control-scrambled peptide SLLK, NS were differentiated in the presence of 50 μg/mL of either of the peptides (GenScript) and replaced every alternate day for 8 days.

qRT-PCR Analysis

cDNA (see Supplemental Experimental Procedures) was subjected for qRT-PCR in triplicates using the 7500 Real-Time PCR system (Applied Biosystems, Foster City, CA, USA), and TaqMan Universal PCR Master Mix (Applied Biosystems) with TaqMan gene expression assays of mouse target genes. Relative expression was calculated by Relative Quantification software (Roche Diagnostics) using β-actin for normalization.

Primers sequences used for amplification were as follows:
TSP1: TaqMan Real-Time ready assay ID: Mm00449020_g1
β-Actin: TaqMan Real-Time ready assay ID: Mm00607939_s1

Immuno Labeling

Immunocytochemistry

Coverslips were washed with PBS, fixed with 2% PFA, and immune labeled as described previously (Zilkha-Falb et al., 2016), except for the additional primary antibodies used, monoclonal anti-NeuN (1:400) and monoclonal anti-TSP1 (1:200). Nuclei were visualized by DAPI counterstaining. Slides were examined using an LSM 510 laser scanning confocal microscope (Carl Zeiss, Jena, Germany). Digital images were acquired using the Zeiss LSM 510 software (magnifications, ×40 or ×63).

Immunoflourescent Staining of Tissue Sections

Free-floating sections of brain were washed twice in PBS followed by blocking in either 3% rabbit (for goat anti-DCX, mouse anti-RIP) or goat serum (for rabbit anti-NG2) depending on primary antibodies used and 0.1% Triton X-100 in PBS for 1 h at room temperature (RT). Sections were stained as described previously (Zilkha-Falb et al., 2016), except for the additional primary antibodies used, mouse anti-TSP1 (1:200), rat anti-BrdU (1:200), mouse anti-RIP (1:100) rat anti-MAC2 (100), and rat anti-CD45 (1:100). For BrdU labeling, sections were primarily incubated with 2N HCl at 37°C for 30 min, and rinsed in 0.1 M (pH 8.5) borate buffer at RT for 10 min, rinsed twice in PBS, blocked and immune labeled. Images were acquired as described above. Confocal Z-stacks were taken, and cell numbers were counted manually.

Quantification

Immunofluorescence data that were collected from three independent repeats of experiment (n = 6 from each) provided an independent sampling. Analysis of qPCR was from three independent repeats. For morphometric analysis, we used repeats from at least three independent experiments with data obtained from six images (of randomly chosen field of view under ×20 objective) for each time point per condition. Statistical significance was assessed by unpaired two-tailed Student's t test (Excel software). p values < 0.05 were considered significant. All data are presented as mean ± standard error. ImageJ densitometry software (version 1.36, NIH, Bethesda, MD, USA) was used for quantification of TSP1 intensity.

SUPPLEMENTAL INFORMATION

Supplemental Information can be found online at https://doi.org/10.1016/j.stemcr.2020.04.005.

AUTHOR CONTRIBUTIONS

R.Z-.F., N.K., and A.B.-N. conceived the study and designed the experiments. R.Z-.F. and N.K. performed the experiments. R.Z-.F. conducted the confocal imaging and analysis. R.Z-.F. and A.B.-N. wrote the manuscript. All authors discussed the results and conclusions and reviewed the manuscript. All authors read and approved the final manuscript.

ACKNOWLEDGMENTS

This paper is dedicated to the memory of A.B.-N., who recently passed away. Ben-Nun was a strong-minded, vigorous, and inspiring scientist in the field of immunology and autoimmunity research. He was a real friend, a very kind and gentle person.

Received: April 18, 2019
Revised: April 15, 2020
Accepted: April 16, 2020
Published: May 14, 2020

REFERENCES

Aharoni, R., Arnon, R., and Eilam, R. (2005). Neurogenesis and neuroprotection induced by peripheral immunomodulatory treatment of experimental autoimmune encephalomyelitis. J. Neurosci. *25*, 8217–8228.

Altman, J., and Das, G.D. (1965). Autoradiographic and histological evidence of postnatal hippocampal neurogenesis in rats. J. Comp. Neurol. *124*, 319–335.

Alvarez-Buylla, A., Seri, B., and Doetsch, F. (2002). Identification of neural stem cells in the adult vertebrate brain. Brain Res. Bull. *57*, 751–758.

Armada-Moreira, A., Ribeiro, F.F., Sebastião, A.M., and Xapelli, S. (2015). Neuroinflammatory modulators of oligodendrogenesis. Neuroimmunol. Neuroinflam. *2*, 263–273.

Bedard, A., Cossette, M., Levesque, M., and Parent, A. (2002). Proliferating cells can differentiate into neurons in the striatum of normal adult monkey. Neurosci. Lett. *328*, 213–216.

Bennett, L., Yang, M., Enikolopov, G., and Iacovitti, L. (2009). Circumventricular organs: a novel site of neural stem cells in the adult brain. Mol. Cell. Neurosci. *41*, 337–347.

Bernier, P.J., Bedard, A., Vinet, J., Levesque, M., and Parent, A. (2002). Newly generated neurons in the amygdala and adjoining cortex of adult primates. Proc. Natl. Acad. Sci. U S A *99*, 11464–11469.

Bifari, F., Decimo, I., Chiamulera, C., Bersan, E., Malpeli, G., Johansson, J., Lisi, V., Bonetti, B., Fumagalli, G., Pizzolo, G., et al. (2009). Novel stem/progenitor cells with neuronal differentiation potential reside in the leptomeningeal niche. J. Cell Mol. Med. *13*, 3195–3208.

Blakemore, W.F., Chari, D.M., Gilson, J.M., and Crang, A.J. (2002). Modelling large areas of demyelination in the rat reveals the potential and possible limitations of transplanted glial cells for remyelination in the CNS. Glia *38*, 155–168.

Brousse, B., Magalon, K., Durbec, P., and Cayre, M. (2015). Region and dynamic specificities of adult neural stem cells and oligodendrocyte precursors in myelin regeneration in the mouse brain. Biol. Open *4*, 980–992.

Buffo, A. (2007). Fate determinant expression in the lesioned brain: Olig2 induction and its implications for neuronal repair. Neurodegener Dis. *4*, 328–332.

Buffo, A., Vosko, M.R., Erturk, D., Hamann, G.F., Jucker, M., Rowitch, D., and Gotz, M. (2005). Expression pattern of the transcription factor Olig2 in response to brain injuries: implications for neuronal repair. Proc. Natl. Acad. Sci. U S A *102*, 18183–18188.

Cerghet, M., Skoff, R.P., Bessert, D., Zhang, Z., Mullins, C., and Ghandour, M.S. (2006). Proliferation and death of oligodendrocytes and myelin proteins are differentially regulated in male and female rodents. J. Neurosci. *26*, 1439–1447.

Chang, A., Nishiyama, A., Peterson, J., Prineas, J., and Trapp, B.D. (2000). NG2-positive oligodendrocyte progenitor cells in adult human brain and multiple sclerosis lesions. J. Neurosci. *20*, 6404–6412.

Chari, D.M., and Blakemore, W.F. (2002). Efficient recolonisation of progenitor-depleted areas of the CNS by adult oligodendrocyte progenitor cells. Glia *37*, 307–313.

Christopherson, K.S., Ullian, E.M., Stokes, C.C., Mullowney, C.E., Hell, J.W., Agah, A., Lawler, J., Mosher, D.F., Bornstein, P., and Barres, B.A. (2005). Thrombospondins are astrocyte-secreted proteins that promote CNS synaptogenesis. Cell *120*, 421–433.

Dimou, L., Simon, C., Kirchhoff, F., Takebayashi, H., and Gotz, M. (2008). Progeny of Olig2-expressing progenitors in the gray and white matter of the adult mouse cerebral cortex. J. Neurosci. *28*, 10434–10442.

Djogo, T., Robins, S.C., Schneider, S., Kryzskaya, D., Liu, X., Mingay, A., Gillon, C.J., Kim, J.H., Storch, K.F., Boehm, U., et al. (2016). Adult NG2-glia are required for median eminence-mediated leptin sensing and body weight control. Cell Metab. *23*, 797–810.

Duncan, I.D., and Radcliff, A.B. (2016). Inherited and acquired disorders of myelin: the underlying myelin pathology. Exp. Neurol. *283*, 452–475.

Emsley, J.G., Mitchell, B.D., Kempermann, G., and Macklis, J.D. (2005). Adult neurogenesis and repair of the adult CNS with neural progenitors, precursors, and stem cells. Prog. Neurobiol. *75*, 321–341.

Falnikar, A., Stratton, J., Lin, R., Andrews, C.E., Tyburski, A., Trovillion, V.A., Gottschalk, C., Ghosh, B., Iacovitti, L., Elliott, M.B., et al. (2018). Differential response in novel stem cell niches of the brain after cervical spinal cord injury and traumatic brain injury. J. Neurotrauma *35*, 2195–2207.

Fancy, S.P., Zhao, C., and Franklin, R.J. (2004). Increased expression of Nkx2.2 and Olig2 identifies reactive oligodendrocyte progenitor cells responding to demyelination in the adult CNS. Mol. Cell Neurosci. *27*, 247–254.

Ganong, W.F. (2000). Circumventricular organs: definition and role in the regulation of endocrine and autonomic function. Clin. Exp. Pharmacol. Physiol. *27*, 422–427.

Gould, E. (2007). How widespread is adult neurogenesis in mammals? Nat. Rev. Neurosci. *8*, 481–488.

Gould, E., Reeves, A.J., Graziano, M.S., and Gross, C.G. (1999). Neurogenesis in the neocortex of adult primates. Science *286*, 548–552.

Gould, E., Vail, N., Wagers, M., and Gross, C.G. (2001). Adult-generated hippocampal and neocortical neurons in macaques have a transient existence. Proc. Natl. Acad. Sci. U S A *98*, 10910–10917.

Horner, P.J., Power, A.E., Kempermann, G., Kuhn, H.G., Palmer, T.D., Winkler, J., Thal, L.J., and Gage, F.H. (2000). Proliferation and differentiation of progenitor cells throughout the intact adult rat spinal cord. J. Neurosci. *20*, 2218–2228.

Jeffery, N.D., Crang, A.J., O'Leary, M.,T., Hodge, S.J., and Blakemore, W.F. (1999). Behavioural consequences of oligodendrocyte progenitor cell transplantation into experimental demyelinating lesions in the rat spinal cord. Eur. J. Neurosci. *11*, 1508–1514.

Kazanis, I., Evans, K.A., Andreopoulou, E., Dimitriou, C., Koutsakis, C., Karadottir, R.T., and Franklin, R.J.M. (2017). Subependymal zone-derived oligodendroblasts respond to focal demyelination but fail to generate myelin in young and aged mice. Stem Cell Rep. *8*, 685–700.

Kohnke, S., Lam, B., Buller, S., Zhao, C., Nuzzaci, D., Tadross, J., Holmqvist, S., Ridley, K., Hathaway, H., Macklin, W., et al. (2019). Nutritional signals rapidly activate oligodendrocyte differentiation in the adult hypothalamic median eminence. bioRxiv, 751198. https://doi.org/10.1101/751198.

Kokoeva, M.V., Yin, H., and Flier, J.S. (2005). Neurogenesis in the hypothalamus of adult mice: potential role in energy balance. Science *310*, 679–683.

Komitova, M., Zhu, X., Serwanski, D.R., and Nishiyama, A. (2009). NG2 cells are distinct from neurogenic cells in the postnatal mouse subventricular zone. J. Comp. Neurol. *512*, 702–716.

Lanz, T.V., Ding, Z., Ho, P.P., Luo, J., Agrawal, A.N., Srinagesh, H., Axtell, R., Zhang, H., Platten, M., Wyss-Coray, T., et al. (2010). Angiotensin II sustains brain inflammation in mice via TGF-beta. J. Clin. Invest. *120*, 2782–2794.

Lassmann, H. (2018). Pathogenic mechanisms associated with different clinical courses of multiple sclerosis. Front. Immunol. *9*, 3116.

Lim, D.A., and Alvarez-Buylla, A. (2016). The adult ventricular-subventricular zone (V-SVZ) and olfactory bulb (OB) neurogenesis. Cold Spring Harb. Perspect. Biol. *8*. https://doi.org/10.1101/cshperspect.a018820.

Lin, R., and Iacovitti, L. (2015). Classic and novel stem cell niches in brain homeostasis and repair. Brain Res. *1628*, 327–342.

Lu, Z., and Kipnis, J. (2010). Thrombospondin 1—a key astrocyte-derived neurogenic factor. FASEB J. *24*, 1925–1934.

Luzzati, F., De Marchis, S., Fasolo, A., and Peretto, P. (2006). Neurogenesis in the caudate nucleus of the adult rabbit. J. Neurosci. *26*, 609–621.

Moyse, E., Segura, S., Liard, O., Mahaut, S., and Mechawar, N. (2008). Microenvironmental determinants of adult neural stem cell proliferation and lineage commitment in the healthy and injured central nervous system. Curr. Stem Cell Res. Ther. *3*, 163–184.

Nait-Oumesmar, B., Picard-Riera, N., Kerninon, C., and Baron-Van Evercooren, A. (2008). The role of SVZ-derived neural precursors in demyelinating diseases: from animal models to multiple sclerosis. J. Neurol. Sci. *265*, 26–31.

Naruse, M., Ishizaki, Y., Ikenaka, K., Tanaka, A., and Hitoshi, S. (2017). Origin of oligodendrocytes in mammalian forebrains: a revised perspective. J. Physiol. Sci. *67*, 63–70.

Picard-Riera, N., Decker, L., Delarasse, C., Goude, K., Nait-Oumesmar, B., Liblau, R., Pham-Dinh, D., and Evercooren, A.B. (2002). Experimental autoimmune encephalomyelitis mobilizes neural progenitors from the subventricular zone to undergo oligodendrogenesis in adult mice. Proc. Natl. Acad. Sci. U S A *99*, 13211–13216.

Pluchino, S., Quattrini, A., Brambilla, E., Gritti, A., Salani, G., Dina, G., Galli, R., Del Carro, U., Amadio, S., Bergami, A., et al. (2003). Injection of adult neurospheres induces recovery in a chronic model of multiple sclerosis. Nature *422*, 688–694.

Redwine, J.M., and Armstrong, R.C. (1998). In vivo proliferation of oligodendrocyte progenitors expressing PDGFalphaR during early remyelination. J. Neurobiol. *37*, 413–428.

Reynolds, R., Cenci di Bello, I., Dawson, M., and Levine, J. (2001). The response of adult oligodendrocyte progenitors to demyelination in EAE. Prog. Brain Res. *132*, 165–174.

Rietze, R., Poulin, P., and Weiss, S. (2000). Mitotically active cells that generate neurons and astrocytes are present in multiple regions of the adult mouse hippocampus. J. Comp. Neurol. *424*, 397–408.

Rivera, J.C., Noueihed, B., Madaan, A., Lahaie, I., Pan, J., Belik, J., and Chemtob, S. (2017). Tetrahydrobiopterin (BH4) deficiency is associated with augmented inflammation and microvascular degeneration in the retina. J. Neuroinflam. *14*, 181.

Robins, S.C., Stewart, I., McNay, D.E., Taylor, V., Giachino, C., Goetz, M., Ninkovic, J., Briancon, N., Maratos-Flier, E., Flier, J.S., et al. (2013a). alpha-Tanycytes of the adult hypothalamic third ventricle include distinct populations of FGF-responsive neural progenitors. Nat. Commun. *4*, 2049.

Robins, S.C., Trudel, E., Rotondi, O., Liu, X., Djogo, T., Kryzskaya, D., Bourque, C.W., and Kokoeva, M.V. (2013b). Evidence for NG2-glia derived, adult-born functional neurons in the hypothalamus. PLoS One *8*, e78236.

Seri, B., Herrera, D.G., Gritti, A., Ferron, S., Collado, L., Vescovi, A., Garcia-Verdugo, J.M., and Alvarez-Buylla, A. (2006). Composition and organization of the SCZ: a large germinal layer containing neural stem cells in the adult mammalian brain. Cereb. Cortex *16* (*Suppl 1*), i103–111.

Serwanski, D.R., Rasmussen, A.L., Brunquell, C.B., Perkins, S.S., and Nishiyama, A. (2018). Sequential contribution of parenchymal and neural stem cell-derived oligodendrocyte precursor cells toward remyelination. Neuroglia *1*, 91–105.

Sim, F.J., Zhao, C., Penderis, J., and Franklin, R.J. (2002). The age-related decrease in CNS remyelination efficiency is attributable to an impairment of both oligodendrocyte progenitor recruitment and differentiation. J. Neurosci. *22*, 2451–2459.

Takemura, N.U. (2005). Evidence for neurogenesis within the white matter beneath the temporal neocortex of the adult rat brain. Neuroscience *134*, 121–132.

Talbott, J.F., Loy, D.N., Liu, Y., Qiu, M.S., Bunge, M.B., Rao, M.S., and Whittemore, S.R. (2005). Endogenous Nkx2.2+/Olig2+ oligodendrocyte precursor cells fail to remyelinate the demyelinated adult rat spinal cord in the absence of astrocytes. Exp. Neurol. *192*, 11–24.

Taupin, P. (2008). Adult neurogenesis, neuroinflammation and therapeutic potential of adult neural stem cells. Int. J. Med. Sci. *5*, 127–132.

Taupin, P. (2006). Neurogenesis in the adult central nervous system. C R. Biol. *329*, 465–475.

Tyzack, G.E., Sitnikov, S., Barson, D., Adams-Carr, K.L., Lau, N.K., Kwok, J.C., Zhao, C., Franklin, R.J., Karadottir, R.T., Fawcett, J.W., et al. (2014). Astrocyte response to motor neuron injury promotes structural synaptic plasticity via STAT3-regulated TSP-1 expression. Nat. Commun. *5*, 4294.

van Tilborg, E., de Theije, C.G.M., van Hal, M., Wagenaar, N., de Vries, L.S., Benders, M.J., Rowitch, D.H., and Nijboer, C.H. (2018). Origin and dynamics of oligodendrocytes in the developing brain: implications for perinatal white matter injury. Glia *66*, 221–238.

Virard, I., Gubkina, O., Alfonsi, F., and Durbec, P. (2008). Characterization of heterogeneous glial cell populations involved in dehydration-induced proliferation in the adult rat neurohypophysis. Neuroscience *151*, 82–91.

Warrington, A.E., Barbarese, E., and Pfeiffer, S.E. (1993). Differential myelinogenic capacity of specific developmental stages of the oligodendrocyte lineage upon transplantation into hypomyelinating hosts. J. Neurosci. Res. *34*, 1–13.

Windrem, M.S., Nunes, M.C., Rashbaum, W.K., Schwartz, T.H., Goodman, R.A., McKhann, G., 2nd, Roy, N.S., and Goldman, S.A. (2004). Fetal and adult human oligodendrocyte progenitor cell isolates myelinate the congenitally dysmyelinated brain. Nat. Med. *10*, 93–97.

Winkler, C.C., Yabut, O.R., Fregoso, S.P., Gomez, H.G., Dwyer, B.E., Pleasure, S.J., and Franco, S.J. (2018). The dorsal wave of neocortical oligodendrogenesis begins embryonically and requires multiple sources of sonic hedgehog. J. Neurosci. *38*, 5237–5250.

Xing, Y.L., Roth, P.T., Stratton, J.A., Chuang, B.H., Danne, J., Ellis, S.L., Ng, S.W., Kilpatrick, T.J., and Merson, T.D. (2014). Adult neural precursor cells from the subventricular zone contribute significantly to oligodendrocyte regeneration and remyelination. J. Neurosci. *34*, 14128–14146.

Xu, Y., Tamamaki, N., Noda, T., Kimura, K., Itokazu, Y., Matsumoto, N., Dezawa, M., and Ide, C. (2005). Neurogenesis in the ependymal layer of the adult rat 3rd ventricle. Exp. Neurol. *192*, 251–264.

Zhao, M., Momma, S., Delfani, K., Carlen, M., Cassidy, R.M., Johansson, C.B., Brismar, H., Shupliakov, O., Frisen, J., and Janson, A.M. (2003). Evidence for neurogenesis in the adult mammalian substantia nigra. Proc. Natl. Acad. Sci. U S A *100*, 7925–7930.

Zilkha-Falb, R., Kaushansky, N., Kawakami, N., and Ben-Nun, A. (2016). Post-CNS-inflammation expression of CXCL12 promotes the endogenous myelin/neuronal repair capacity following spontaneous recovery from multiple sclerosis-like disease. J. Neuroinflam. *13*, 7.

Stem Cell Reports, Volume *14*

Supplemental Information

The Median Eminence, A New Oligodendrogenic Niche in the Adult Mouse Brain

Rina Zilkha-Falb, Nathali Kaushansky, and Avraham Ben-Nun

Supplemental information

Supplementary figures and legends

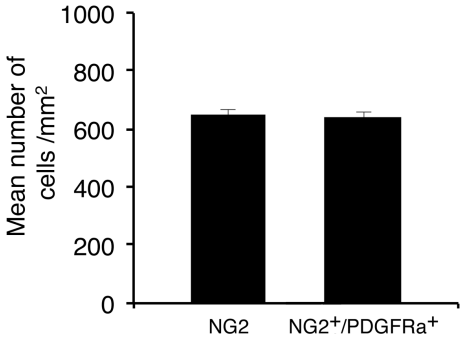

Figure S1 Quantitative analysis of $NG2^+$ and $NG2^+/PDGFRa^+$ in the ME of naïve mice calculated as mean number of marker/s positive cells per mm^2, (n=4 for each group).

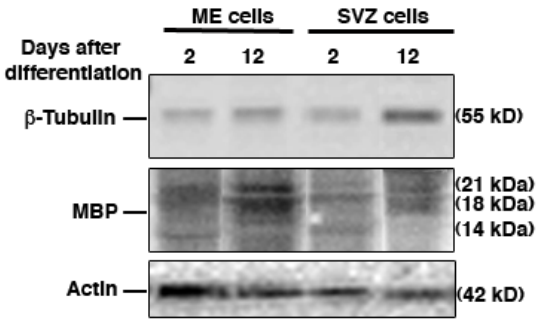

Figure S2 Western blot analysis of neuronal (b-Tubulin) and oligodendrocyte (MBP) markers following differentiation of ME- or SVZ-NSCs.

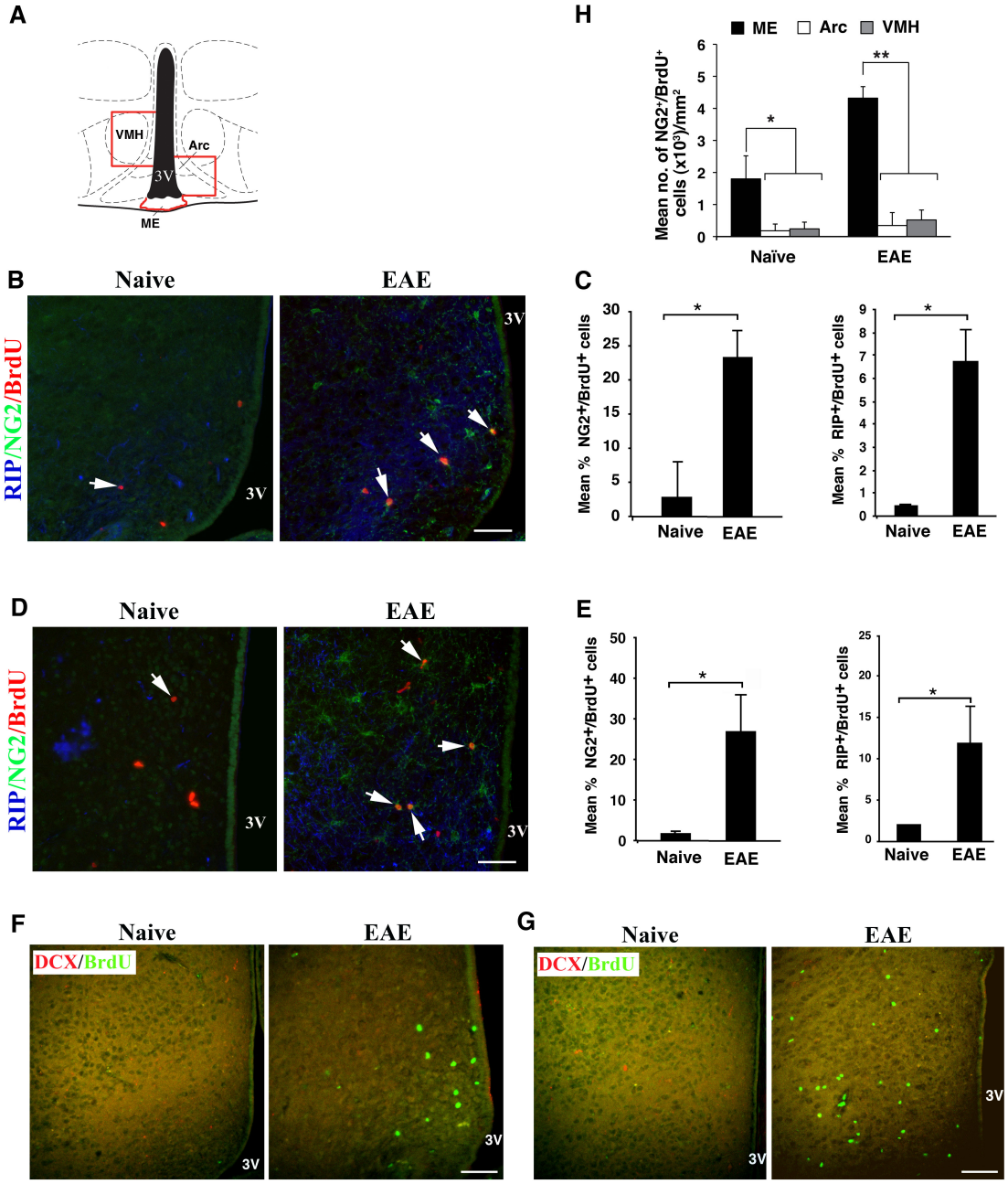

Figure S3 EAE induces oligodendrogenesis in the Arc and VMH of the hypothalamus (**A**) Schematic draw of the hypothalamus regions that were analyzed (**B**) Confocal images of double staining $NG2^+/BrdU^+$ and $RIP^+/BrdU^+$ in the Arc. bar=50μm. (**C**) Quantitative analysis of $NG2^+/BrdU^+$ and $RIP^+/BrdU^+$ in the Arc**.** Left: *p≤0.006, right: *p=0.03 **(D)** Confocal images of double staining $NG2^+/BrdU^+$ or $RIP^+/BrdU^+$ in the VMH. bar=50μm. (**E**) Quantitative analysis of $NG2^+/BrdU^+$ in the VMH *p=0.03, Two-tails student T test. **(F)** Images show no DCX staining in Arc in naïve and EAE

mice. bar=50μm. **(G)** Images show no DCX staining in VMH in naïve and EAE mice. bar=50μm. (H) Quantitative analysis of percentage of $NG2^{+}/BrdU^{+}$ cells in ME compare Arc and VMH in Naïve and EAE mice (n=4) ; * p=0.04 ; ** p=0.01.

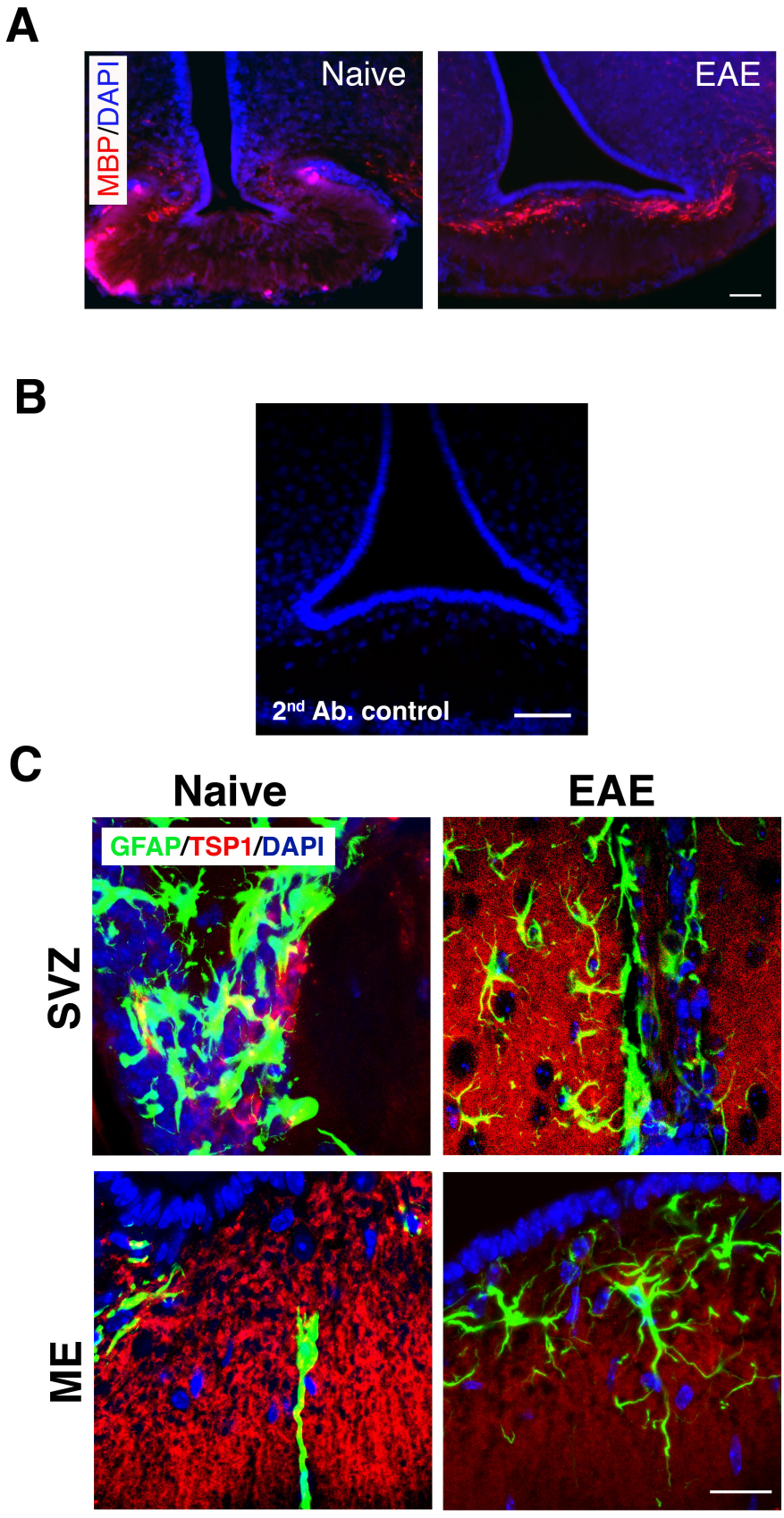

Figure S4 (A) MBP immunostaining in ME of naïve and EAE mice. bar=50μm.

(B) Negative control staining with only secondary antibody (**C**) Low power images of TSP1 from sections shown in Fig. 4F. bar=50μm.

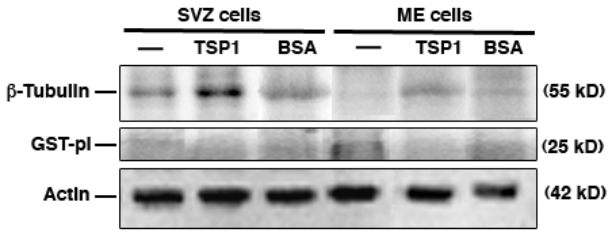

Figure S5 Western blot analysis of neuronal (b-Tubulin) and oligodendrocyte (GST-pI) markers following differentiation of ME- or SVZ-NSCs in presence of TSP1.

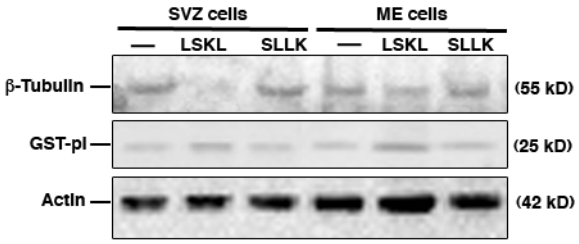

Figure S6 Western blot analysis of neuronal (b-Tubulin) and oligodendrocyte (GST-pI) markers following differentiation of ME- or SVZ-NSCs in presence of TSP1 antagonist (LSKL) or agonist (SLLK).

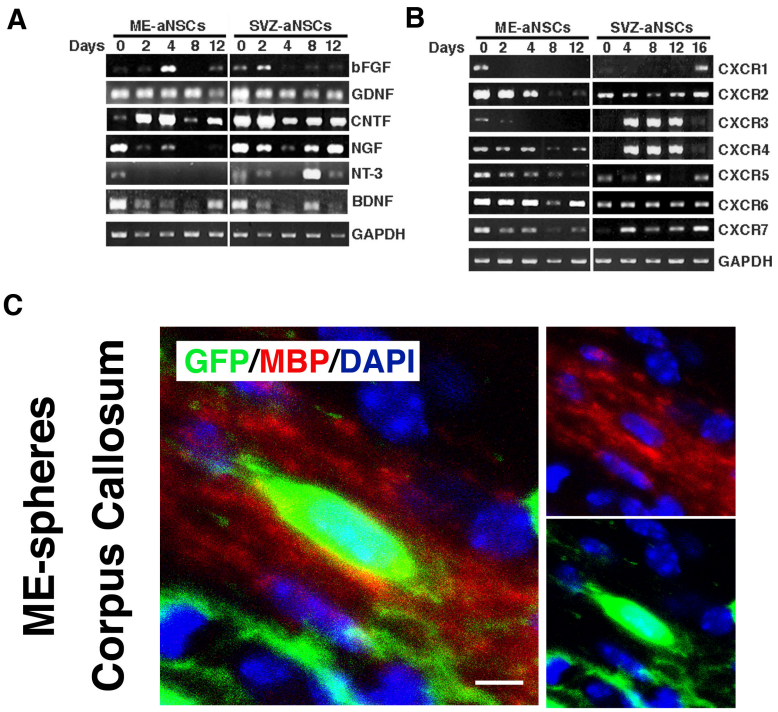

Figure S7 temporal expression profile of chemokine receptors **(A)** and neurotrophic factors **(B)** by ME-originated cells are distinct from these expressed by SVZ-originated cells. Semiquantitative RT–PCR of cDNA reverse transcribed from total RNA extracted from ME-NSCs compare SVZ-NSCs at elevated time points following differentiation. Undifferentiated NSCs (day 0) served as control. GAPDH expression was assessed as an internal standard. Results are representative of three repeats. **(C)** Single GFP^+/MBP^+ cell derived from ME-NS in the CC demonstrating short MBP-positive profiles at the periphery of the GFP-positive soma. bar=20μm.

Supplemental table 1

List of used antibodies

Antibody	Manufacture	Cat. No.
mouse anti-glial fibrillary acidic protein (GFAP)	Sigma	G-3893
monoclonal mouse anti-NeuN	Chemicon	MAB377
rat anti-MBP	Chemicon	MAB386
rabbit anti-NF200	Sigma	N4142
goat anti-DCX	Chemicon	Sc-8066
monoclonal mouse anti β-Tubulin III	Chemicon	MAB1637
rabbit anti NG2	Chemicon	AB5320
rat anti BrdU	Serotec	MCA2060
rat anti-platelet derived growth factor alpha (PDGFRa)	eBioscience	14-1401
rat anti MAC2	Biolegend	125401
rat anti CD45	Biolegend	103101

Supplementary methods

Semiquantitative RT-PCR analysis. Total RNA was purified either from NSCs at time point 0 (undifferentiated NSCs) or from NSCs which were cultured in differentiation medium on PDL for elevated time points, using TRIzol Reagent (Invitrogen Corp.). cDNA was prepared from 1 μg of total RNA using MMLV-

reverse transcriptase (Promega, Madison, WI) and olido-dT (Promega, Madison, WI) according to manufacturer's instructions. The cDNA mixure was diluted 1:5 with PCR-grade water. We examined the expression of specific mRNAs using semi-quantitative reverse transcription PCR (RT-PCR) with selected gene-specific primer pairs. The primers used were: TSP1, sense 5'- CAA GGG CTCAGGGATACTCAGG-3', antisense 5'- AGG TTT TGT CAT AGA TGG GTC C-3' (product size, 270 bp); CXCR1, sense 5'- GGC CGA GGC TGA ATA TTT CAT TCT-3', antisense 5'- GGT GGC ATG GAC GAT GGC CAG TAT-3' (product size, 450 bp); CXCR2, sense 5'- GGA GAA TTC AAG GTG GAT AAG-3', antisense 5'- AGT GTC TCT TCT GGA TCA GTG-3' (product size, 486 bp); CXCR3, sense 5'- GAG GTT AGT GAA CGT CAA GTG-3', antisense 5'- GGG GTC CCT GCG GTA GAT CTG-3' (product size, 482 bp); CXCR4, sense 5'- GGT CTG GAG ACT ATG ACT CC-3', antisense 5'- CAC AGA TGT ACC TGT CAT CC-3' (product size, 525 bp); CXCR6, sense 5'- ACA AAG ATG TTG CTG GCA GA-3', antisense 5'-GGC CTG TTT TCA GTC CCA TA-3' (product size, 219 bp); CXCR7, sense 5'- TTT GAG TTC AGG GGA GGA T-3', antisense 5'-GCT CGC TGA CAC CTA ACC TC-3' (product size, 202 bp); CCR1, sense 5'- ATG GAG ATT TCA GAT TTC ACA GAA-3', antisense 5'- GGC TAC AGG TAC GGT GAG TGA ACT-3' (product size, 510 bp); CCR2, sense 5'- ATG TTA CCT CAG TTC ATC CAC GGC-3', antisense 5'- GTA ATG GTG ATC ATC TTG TTT GGA-3' (product size, 506 bp); CCR3, sense 5'- ATG GCA TTC AAC ACA GAT GAA-3', antisense 5'- GTC ACA GTT CGG GCT CGA AGG-3' (product size, 512 bp); and GAPDH, sense 5'- CCA TCA ACG ACC CCT TCA TTG AC-3', antisense 5'- GGA TGA CCT TGC CCA CAG CCT TG-3' (product size, 580 bp).

The RT-PCR reactions were carried out using 100 ng of cDNA, 20 pmol of each primer, and Taq polymerase (Sigma-Aldrich, Israel) in a total volume of 20 ml. PCR reactions were carried out in a PTC-100 programmable Thermal controller (MJ Research, Inc) PCR system. Amplification included one stage of 5 min at 95ºC followed by 35 cycles of 95ºC for 30 s, 56ºC for 1 min, 72ºC for 1 min and 72ºC for 10 min then reactions were kept at 4ºC. As an internal standard for the amount of cDNA synthesized, we used GAPDH mRNA. PCR products were subjected to agarose gel analysis and visualized by ethidium bromide staining. In all cases one product was observed with each primer set, and the observed product had an amplicon size predicted from published cDNA sequences.

Western blot

Cells were lysed (25 mM Tris–HCl pH 7.6, 150 mM NaCl, 1 mM EDTA, 1% Triton X-100, 1 mM Na3VO4, 100 nM, PMSF and protease inhibitor cocktail (1:50; Sigma--Aldrich). Lysis was done 1h/4°C then lysate was centrifuged 13,000rpm/30min/4°C and supernatant was collected. The protein content of cell lysates was determined using the BCA protein estimation kit (Pierce; Rockford, IL) with BSA as a standard. Proteins were denatured at 95°C for 5 minutes and further diluted in sample buffer (250 mM Tris-HCl pH 6.8 containing 4% SDS, 10% glycerol and 2% β-mercaptoethanol). Equal amounts of proteins were resolved on 10% SDS-PAGE and transferred onto nitrocellulose membrane (Invitrogen kit) for subsequent immuno-blotting with antibodies specific for Tubulin beta (1:1000; Chemicon), MBP (1:2000; Chemicon), GST-pI (1:3000; Abcam). To control protein loading, blots were additionally stained with either anti-β-actin (1:5000; Abcam). Blots were analyzed by standard chemi-luminescence (Supersignal Kit, Pierce, Rockford, IL, USA) and visualization was done by a ChemiDoc™ XRS System (Bio-Rad).